Role of the [4Fe-4S] Cluster in Reductive Activation of the Cobalt Center of the Corrinoid Iron−Sulfur Protein from *Clostridium thermoaceticum* during Acetate Biosynthesis†

Saurabh Menon and Stephen W. Ragsdale*

Department of Biochemistry, Beadle Center, University of Nebraska, Lincoln, Nebraska 68588-0664

Received November 14, 1997; Revised Manuscript Received February 11, 1998

ABSTRACT: The corrinoid iron−sulfur protein (CFeSP) from *Clostridium thermoaceticum* functions as a methyl carrier in the Wood−Ljungdahl pathway of acetyl-CoA synthesis. The small subunit (33 kDa) contains cobalt in a corrinoid cofactor, and the large subunit (55 kDa) contains a [4Fe-4S] cluster. The cobalt center is methylated by methyltetrahydrofolate (CH_3-H_4folate) to form a methylcobalt intermediate and, subsequently, is demethylated by carbon monoxide dehydrogenase/acetyl-CoA synthase (CODH/ACS). The work described here demonstrates that the [4Fe-4S] cluster is required to facilitate the reactivation of oxidatively inactivated Cob(II)amide to the active Co(I) state. Site-directed mutagenesis of the large subunit gene was used to change residue 20 from cysteine to alanine, which resulted in formation of a cluster with EPR and redox properties consistent with those of [3Fe-4S] clusters. The midpoint potential of the cluster in the C20A variant was ∼500 mV more positive than that of the [4Fe-4S] cluster in the native enzyme. Accordingly, it was found that the Co center in the C20A mutant protein could be reduced artificially but was severely crippled in its ability to be reduced by physiological electron donors. This is probably because the reduced cluster of the C20A protein cannot provide the driving force needed to reduce Co(II) to Co(I), since the Co(II/I) midpoint potential is −504 mV. The C20A variant also was unable to catalyze the steady-state synthesis of acetyl-CoA when CH_3-H_4folate or methyl iodide were provided as methyl donors and CO and CODH/ACS as reductants. Addition of chemical reductants rescued the catalytically crippled variant form in both of these reactions. On the other hand, in single-turnover reactions, the methyl−Co state of the altered protein was fully active in methylating H_4folate and in synthesizing acetyl-CoA in the presence of CO and CoA. The combined results strongly indicate that the FeS cluster of the CFeSP is necessary for reductive activation of Co(II) to Co(I) by physiological reductants but is not required for catalysis, e.g., demethylation of CH_3-H_4folate or methylation of CODH/ACS. We propose that, during reductive activation, electrons flow from the reduced electron-transfer protein (e.g., CODH/ACS or reduced ferredoxin (Fd)) to the FeS cluster which then directs electrons to the cobalt center for catalysis. These results also support earlier hypotheses that the methylation and demethylation reactions involving the CFeSP are S_N2-type nucleophilic displacement reactions and do not involve radical chemistry.

Acetogenic bacteria and methanogenic archea can synthesize all of their macromolecules from H_2 and CO_2 (*1*−*4*). The key steps in autotrophic growth involve the synthesis of the acetyl group of acetyl-CoA from 2 mol of CO_2 by the Wood−Ljungdahl pathway (*5*, *6*). One mole of CO_2 is converted to the methyl group and the other to the carbonyl group of acetyl-CoA, which is the building block for further biosynthetic reactions. The Wood−Ljungdahl pathway is also used by acetogens to convert six-carbon sugars into 3, instead of 2, mol of acetyl-CoA/mol of hexose fermented. Acetoclastic methanogens use the reverse of this pathway to convert acetate to CO_2 and methane. The Wood−Ljungdahl pathway has been most thoroughly studied with the acetogenic bacterium *Clostridium thermoaceticum*. Two key steps involve a corrinoid iron−sulfur protein (CFeSP).[1] The first is a reaction catalyzed by CH_3-H_4folate/CFeSP methyltransferase (MeTr) in which the CFeSP accepts the N-5 methyl group of CH_3-H_4folate to form bound methylcobamide (eq 1). Then, in a subsequent reaction that does not involve MeTr, the methyl group is transferred from

$$CH_3\text{-}H_4\text{folate} + H^+ + \text{Co(I)}-\text{CFeSP} \rightarrow CH_3\text{-Co(III)}-\text{CFeSP} + H_4\text{folate} \quad (1)$$

$$CH_3\text{-Co(III)}-\text{CFeSP} + \text{ACS} \rightleftharpoons CH_3-\text{ACS} + \text{Co(I)}-\text{CFeSP} \quad (2)$$

$$\text{Co(I)}-\text{CFeSP} \rightleftharpoons \text{Co(II)}-\text{CFeSP} + 1e^- \quad (3)$$

† This work was supported by NIH Grant GM39541 (to S.W.R.).

* To whom correspondence should be addressed. Phone: 402-472-2943. Fax: 402-472-7842. E-mail: sragsdal@unlinfo.unl.edu.

[1] Abbreviations: CFeSP, corrinoid iron sulfur protein; SDS−PAGE, sodium dodecyl sulfate−polyacrylamide gel electrophoresis; CODH/ACS, CO dehydrogenase/acetyl-CoA synthase; MeTr, CH_3-H_4folate, methyltetrahydrofolate; PFOR, pyruvate/ferredoxin oxidoreductase; DTT, dithiothreitol; AdoMet, *S*-adenosyl-L-methionine; CAPS, 3-(cyclohexylamino)-1-propanesulfonate; Fd, ferredoxin.

S0006-2960(97)02799-2 CCC: $15.00 © 1998 American Chemical Society
Published on Web 03/27/1998

methylcobalt to carbon monoxide dehydrogenase/acetyl-CoA synthase (CODH/ACS) (*7*) to form a methylmetal adduct at a unique metal center on the ACS subunit (eq 2).

The CFeSP from *C. thermoaceticum* was first isolated in 1984 (*8*). It was shown to be an 88 kDa heterodimeric protein with 55 and 33 kDa subunits and demonstrated to catalyze reaction 1. When the CFeSP was purified to homogeneity, its bound corrinoid cofactor was identified to be a vitamin B_{12} derivative, 5-methoxybenzimidazolylcobamide; in addition, a component [4Fe-4S] cluster was discovered (*9*). This was the first published example of a corrinoid protein with an iron−sulfur cluster. The large 55 kDa subunit was shown to contain the cluster and the small subunit to house the corrinoid (*10*). A similar CFeSP has been found in acetoclastic methanoarchaea as a component of a multienzyme complex that is involved in converting acetyl-CoA to methane (*11*). The physical properties of the methanogenic CFeSP were found to be highly similar to those of the protein from acetogenic bacteria (*12*).

The genes encoding the large and small subunits of the CFeSP were cloned and found to be part of a large gene cluster that also contains the MeTr and CODH/ACS genes (*13*). When the CFeSP genes were sequenced and the protein was heterologously expressed, it was found that *E. coli* was unable to synthesize active protein (*10*). Generation of the active recombinant protein required unfolding, refolding, and reconstitution of the cofactors. The reconstituted protein was found to be identical in its spectroscopic and kinetic properties to the native CFeSP from *C. thermoaceticum* (*10*). These studies demonstrated that the heterologous expression system could be used to produce CFeSP and that site-directed mutation of the CFeSP gene was a feasible approach to probe structure and mechanism.

As indicated by Figure 1 and eqs 1 and 2, the CFeSP cycles between the Co(I) and the methyl−Co(III) states during catalysis. These are not viewed to be redox reactions but S_N2 displacement reactions involving, in eq 1, nucleophilic attack by Co(I) on the electrophilic methyl group attached to the N-5 position of H_4folate and, in eq 2, nucleophilic displacement of a methyl cation by a metal center on CODH/ACS. It has been considered, based on biomimetic models of the methyl group transfer from the CFeSP to ACS (*14*, *15*), that reaction 2 could involve redox chemistry and methyl radical transfer; however, the nonredox transfer of a methyl cation has remained the favored mechanism (discussed in (*7*, *16*)). Therefore, the role during catalytic turnover for a cofactor that typically performs redox reactions, e.g., the [4Fe-4S] cluster, was not apparent.

A possible role for the cluster is to facilitate reductive activation of the CFeSP. A proposed activation cycle based on the results reported here is outlined in Figure 1. The Co(II/I) redox couple has a very low midpoint potential of −504 mV (*17*), and the Co(II) state is not active in methyl transfer reactions (*18*, *19*). Although the ambient redox potential in growing anaerobic acetogenic cells is not known, it is likely that conditions in the cell are favorable for Co(I) to periodically escape from the catalytic cycle by one-electron oxidation to the inactive Co(II) state. Re-entry into the catalytic cycle then requires reductive activation by low-potential electrons. CO in the presence of CODH/ACS or pyruvate/ferredoxin oxidoreductase (PFOR) in the presence of pyruvate and CoA has been shown to reduce the CFeSP;

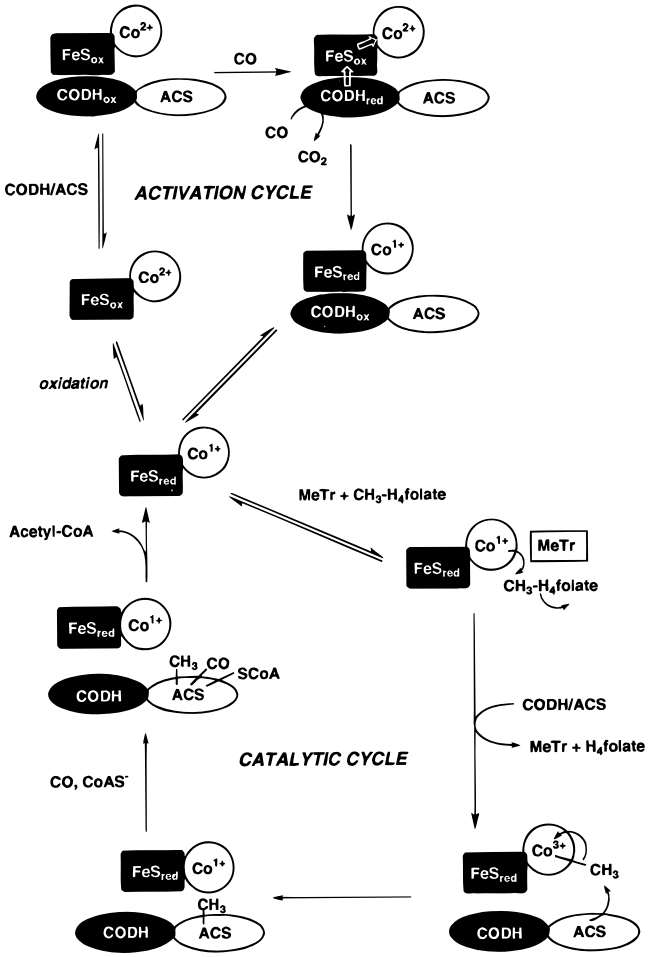

FIGURE 1: Activation and catalytic cycles involving the CFeSP. Since Fd increases the rate of electron transfer from CODH/ACS to the CFeSP, a ternary complex involving CODH/ACS, Fd, and CFeSP could also be drawn; however, the scheme is simplifed by excluding Fd.

Fd enhances the rate of reduction by ∼3-fold (*9*). The midpoint potential for the 2+/1+ couple of the [4Fe-4S] cluster (−523 mV) is even lower than that of the Co(II/I) couple (*17*), which is consistent with a role in electron transfer to the cobalt center. More direct evidence for the cluster's requirement in reduction of Co(II) to Co(I) was provided by chemical modification studies using mersalyl acid to disrupt the FeS cluster. The mersalyl-treated CFeSP could not be methylated by CH_3-H_4folate in the presence of MeTr, CODH/ACS, and CO (*9*).

Our working hypothesis was that the cluster was involved in transferring electrons from external donors to Co, thus facilitating the reductive activation of inactive Co(II) to Co(I). To determine the function of the iron−sulfur cluster in catalysis and/or reductive activation, we altered one of the cysteine residues that was a likely iron ligand to alanine in order to convert the [4Fe-4S] cluster into a [3Fe-4S] cluster. The rationale was that, since the midpoint potentials for [3Fe-4S]$^{+/0}$ couples are generally much more positive than those for [4Fe-4S]$^{2+/+}$ clusters (*20*), the reduced 3Fe cluster would not be a strong enough electron donor to reduce the cobalt center. Thus, a [3Fe-4S] containing CFeSP would be expected to be crippled in reactions at cobalt that require redox chemistry. Our results strongly support our hypothesis that the [4Fe-4S] cluster plays a key role in reductive

activation of the Co center. Our results also provide further evidence that the cobalt center cycles through the Co(I) and methyl−Co(III) states and that methylation of the CFeSP by CH_3-H_4folate and the methylation of CODH/ACS by the methylated CFeSP involves S_N2 chemistry.

MATERIALS AND METHODS

Materials. N_2 (99.98%) and CO (99.99%) were obtained from Linweld (Lincoln, NE). N_2 was deoxygenated by passing through a heated column containing BASF catalyst. Reagents were of the highest purity available.

Organism and Enzyme Purification. *Escherichia coli* strain JM109 was grown at 37 °C on LB medium supplemented with 0.2 mM IPTG. *C. thermoaceticum* strain ATCC 39073 was grown on glucose at 55 °C (*21*). The CFeSP from *C. thermoaceticum* was purified under strictly anaerobic conditions as described (*9*). Purification of the C20A CFeSP variant is described below. CODH/ACS (*22*), Fd II (*23*), and MeTr (*19*) were purified as described under strictly anaerobic conditions at 17 °C in a Vacuum Atmospheres chamber maintained below 1 ppm oxygen. Protein concentrations were determined by the Rose Bengal method (*24*).

Construction of the C20A Mutant. The gene (acsC) encoding the large subunit of the CFeSP (*13*) had previously been inserted as an NdeI-Hind III fragment into plasmid pET946B55 (*10*). Plasmid pET946B55 was transformed into competent JM109 cells and the plasmid DNA was isolated. Near the N-terminus of the large subunit of the CFeSP, there are three cysteine residues that are spaced in a manner that strongly suggested that they might serve as ligands for the [4Fe-4S] cluster. We decided to use site-directed mutagenesis to change the second cysteine residue in this group (at position 20) to alanine. The strategy was to use PCR methods to generate and amplify a PCR fragment that would include the DNA encoding the cysteine block and to switch this region of the wild-type gene with the PCR fragment. Site-directed mutagenesis was performed using the overlap extension PCR protocol (*25*) using primers 1−4 which were synthesized. Two PCR reactions were first run−one using primers 1 and 2, and the other with primers 3 and 4 using

Primer 1: GTGGCGAGGCCCGGGACACCC

Primer 2: CCCCCATTTCTACGGCAGTCGG

Primer 3: GGGTGTCCCGGCCTCGCCAC

Primer 4: TTAATACGACTCACTATAGGG.

the plasmid DNA from pET946B55 as a template. The mutagenic primer was primer 1 (the underlined nucleotides denote the site of the mutation). These reactions yielded two 165 bp fragments that were then used as templates in a PCR reaction to generate and amplify a 330 bp product that would correspond to part of the pET plasmid and to residues 1−77 of the protein sequence. The sequence of the 330 bp product was confirmed by DNA sequence analysis. This 330 bp fragment containing the mutation was isolated by electrophoresis on a 3% agarose gel, excised, treated with β-agarase, and cloned into a TA vector according to the instructions of the manufacturer (Invitrogen). Transformants were selected by blue/white colony screening, confirmed for the presence of the correct insert by performing restriction digestions with NotI and NdeI, and the DNA was isolated. The TA cloning vector was then digested with NdeI and NotI and inserted into the NdeI and NotI sites of pET946B55. Plasmid pET946B55 was transformed into Bl-21(DE1) cells from Novagen which was grown aerobically on LB-ampicillin medium at 27 °C to maximize the amount of soluble large subunit. The previously constructed $pSCP_3$ (*10*), which contains the small subunit of the CFeSP (acsD), was then transformed into *E. coli* HB101 cells which were grown at 37 °C on LB medium supplemented with 0.1 mg mL^{-1} of ampicillin. IPTG (0.2 mM) was added during the log phase of growth to induce expression of acsD at a level of ∼30% of cell protein.

Reconstitution and Purification of the Recombinant CFeSP. Reconstitution of the C20A variant was performed by modifying a previously published procedure for the recombinant wild-type CFeSP (*10*). The strategy involved separately expressing the two recombinant subunits and then reconstituting the dimeric protein with cofactors. Four hours after 0.2 mM IPTG was added to the BL21 cells containing acsC, when the absorbance value at 600 nm of the culture had reached ∼2.0, the cells were centrifuged, suspended in 50 mM Tris-HCl buffer, pH 7.6, 2 mM dithiothreitol (DTT), and lysed using a Heat Systems Xl sonicator inside a Coy Products (Ann Arbor, MI) anaerobic chamber. The lysate was then loaded anaerobically into centrifuge tubes and centrifuged in a type 35 rotor at 30 000 rpm for 1 h. The supernatant fraction was suspended in a solution containing 6 M urea, 300 μmol DTT, 3 μmol Na_2S, and 3 μmol ferrous ammonium sulfate.

The HB101 cells overexpressing acsD were grown to an absorbance of ∼2.0, centrifuged, and lysed as described above, and 3 μmol of hydroxocobalamin was added to the lysate. This solution was then added to the soluble fraction from the BL21 lysate to give a final urea concentration of 4 M. This solution was then diluted 10-fold with a solution containing 50 mM Tris-HCl, pH 7.6, 2 mM dithiothreitol, and 3 μmol hydroxocobalamin to decrease the urea concentration to 0.4 M. After incubation for 4 h, the solution was centrifuged to remove the precipitated protein and then concentrated with a Amicon ultrafiltration unit containing a YM30 membrane. The reconstituted mixture was then applied to a 100 mL DEAE Sephacel column and eluted with a gradient from 0 to 0.6 M NaCl in 50 mM Tris-HCl, pH 7.6. Fractions were combined on the basis of the intensity of the red color of the cobamide and analysis by SDS polyacrylamide gel electrophoresis. Ammonium sulfate was added to the combined fractions to 0.8 M, and the solution was applied to a phenyl Sepharose column equilibrated with 0.8 M ammonium sulfate in 50 mM Tris-HCl, pH 7.6, and 2 mM DTT. The reconstituted CFeSP was then eluted with a reverse gradient from 0.8 to 0 M ammonium sulfate in the same buffer.

EPR and Circular Dichroism (CD) Spectroscopy and Spectroelectrochemistry. EPR spectra were recorded on a Bruker ESP 300E spectrometer equipped with an Oxford ITC4 temperature controller, a model 5340 automatic frequency counter (Hewlett-Packard), and Bruker gaussmeter. Spin concentrations were measured by comparing the double integrals of the spectra with those of a 1 mM copper perchlorate standard. CD measurements were made at 25 °C on a Olis-RSM CD system equipped with a DeSa monochromator and a Xenon Arc lamp.

For the EPR spectroelectrochemistry experiments, a solution (final volume of 0.6 mL) containing CFeSP (50 μM, final) was added to an EPR electrochemical cell (*26*) in the anaerobic chamber, and the following redox mediators were added to a final concentration of 50 μM: thionine (+80 mV), methylene blue (+11 mV), indigotetrasulfonate (−46 mV), indigodisulfonate (−125 mV), and anthraquinone-1,5-disulfonate (−170 mV). Equilibrium was considered to be obtained when the measured potential drift was 2−3 mV in 5 min. To ensure that radical signals from the mediators did not interfere with the cluster EPR spectrum, the spectra of an identical mediator mix in the absence of the protein was first recorded at same redox potentials. Minor signals from the cavity at all potentials and presumably derived from thionine at potentials between +50 and +10 mV were subtracted (using supplied Bruker software) from the spectra of the protein sample at the same potentials.

Corrinoid Determination. The concentration of corrinoid in the protein was measured by conversion to the dicyano derivative by a modification of the procedure described before (*27*). The CFeSP (5−10 μL) was added to a 0.5 mL solution in a 1.5 mL eppendorf tube containing 50 mM 3-(cyclohexylamino)-1-propanesulfonate (CAPS), pH 10, and 20 mM potassium cyanide. The solution was heated for 5 min at 90 °C and allowed to cool to room temperature. The concentration of corrinoid was measured by determining the absorbance values at 369 and 584 nm, where the extinction coefficients are 31.1 and 11 mM^{-1} cm^{-1} (*27*). A control spectrum lacking protein served as the reference spectrum.

Enzyme Assays. The reduction of Co(II) to Co(I) by CODH/ACS and CO was performed in a 2 mL (final volume) reaction mixture containing 0.5 μM CODH/ACS and 5 μM CFeSP in 50 mM Tris-HCl, pH 7.6. The rate of reduction of Co(II) was followed by monitoring the appearance of the 390 nm peak of Cob(I)amide. Since the rate of reduction of the C20A variant is extremely slow, the reaction was performed at 55 °C; however, reduction of the wild-type enzyme was monitored at 25 °C since this reaction is relatively fast with equivalent concentrations of CODH. The rate of formation of the Co(I) species for the wild-type enzyme was also monitored at 390 nm at 55 °C with an 8-fold lower concentration of CODH/ACS (62.5 nM). CODH/ACS became inactivated during the long times required to reduce the C20A variant; therefore, the assay mix was checked every 0.5 h for CODH/ACS activity. When the CODH was determined to be inactive, another 1 nmol aliquot of CODH was added.

The reaction of CH_3-H_4folate, CO, and CoA to form acetyl-CoA was conducted under conditions in which either MeTr or CODH/ACS was rate limiting as described previously (*28*). The reaction was performed in the dark in a glass V-shaped reaction vial capped with a red rubber serum stopper. When CODH/ACS was rate limiting, the reaction mixture (25 μL, total volume) contained 4 μg (0.028 nmol) of CODH/ACS, 1.5 μg (0.028 nmol) of MeTr, 50 μg (0.58 nmol) of CFeSP, 0.5 μg (0.083 nmol) of Fd, and 260 nmol CoA in Tris-maleate buffer, pH 5.8. After the mixture was equilibrated with CO and placed in a heating block for 2 min at 55 °C, the reaction was initiated with 100 nmol of $^{14}CH_3$-H_4folate (1000 dpm $nmol^{-1}$) (Amersham Life Sciences). The reaction was quenched at various times by removing 5 μL aliquots into 5 μL of 2.2 N perchloric acid. The amount of acetyl-CoA formed was measured by Dowex 50W-H^+ chromatography as described (*29*). When MeTr was rate limiting, the reaction mixture contained 0.015 nmol of MeTr, 0.50 nmol of CODH/ACS, 0.58 nmol of C/Fe SP, 0.083 nmol of Fd, and 260 nmol of CoA in Tris-maleate buffer, pH 5.8. Other conditions and determination of the amount of acetyl-CoA were as described for the reaction with limiting CODH.

The assay for the synthesis of acetyl-CoA from CH_3I, CoA, and CO was performed in the dark in a glass V-shaped reaction vial capped with a red rubber serum stopper. The reaction was carried out at 25 °C instead of 55 °C because of the low boiling point of CH_3I. The conditions were the same as for the synthesis of acetyl-CoA from CH_3-H_4folate but CH_3I replaced MeTr and CH_3-H_4folate. After being bubbled with CO for 5 min, the reaction mixture was equilibrated at 25 °C and the reaction was initiated by adding $^{14}CH_3I$ (3200 dpm/nmol). The reaction was terminated by removing 5 μL aliquots at various time points into 5 μL of 2.2 N perchloric acid as above. The aliquots were then heated at 65 °C for 5 min to remove unreacted CH_3I, and the amount of radioactivity was determined by liquid scintillation counting.

CFeSP methylation and the assay for acetyl-CoA synthesis from the methylated CFeSP, CoA, and CO were performed in the dark inside the anaerobic chamber in glass V-shaped reaction vials capped with red rubber serum stoppers. To methylate the CFeSP, the as-isolated protein was reduced by reaction with 10 mM titanium(III) citrate, incubated for 15−30 min at 13 °C with a 20-fold excess of $^{14}CH_3I$, and centrifuged through a Sephadex G-50 column (*30*) to remove the unreacted methyl iodide and the titanium citrate. Then the acetyl-CoA synthesis reaction was performed in a final reaction volume of 25 μL containing 0.028 nmol of CODH/ACS, 0.083 nmol of Fd, 0.58 nmol of methylated CFeSP (3200 dpm $nmol^{-1}$), and 260 nmol of CoA in Tris-maleate buffer, pH 5.8. After the mixture was bubbled with CO for 2 min, the reaction mixture was incubated at 25 °C, and at various times, 5 μL aliquots were removed into an eppendorf tube containing 3 μL of 2.2 N perchloric acid to quench the reaction. The amount of acetyl-CoA was analyzed by Dowex 50W-H^+ chromatography.

The assay for the demethylation of CH_3−CFeSP by H_4-folate was performed in a reaction mix containing 125 nmol of H_4 folate, 12.5 nmol of $^{14}CH_3$-CFeSP (prepared as described above), and 4.6 nmol of MeTr in 50 mM Tris-maleate buffer, pH 5.8, in a final volume of 125 μL. At various times, samples were removed into an eppendorf tube containing 25 μL of 2.2 N perchloric acid to quench the reaction. Sodium hydroxide was added to neutralize the solution, the reaction mixture was then applied to a 0.8 × 8 cm Dowex-1-formate column, and CH_3-H_4folate was eluted as described (*8*).

RESULTS

UV−Visible Spectroscopy. The visible spectra of the C20A variant were very similar to the wild type in the three oxidation states (Figure 2) (*9*). They are comprised of various charge-transfer bands from the cobamide and the [4Fe-4S] cluster. The amount of corrinoid in the C20A protein was determined as the dicyano derivative. The

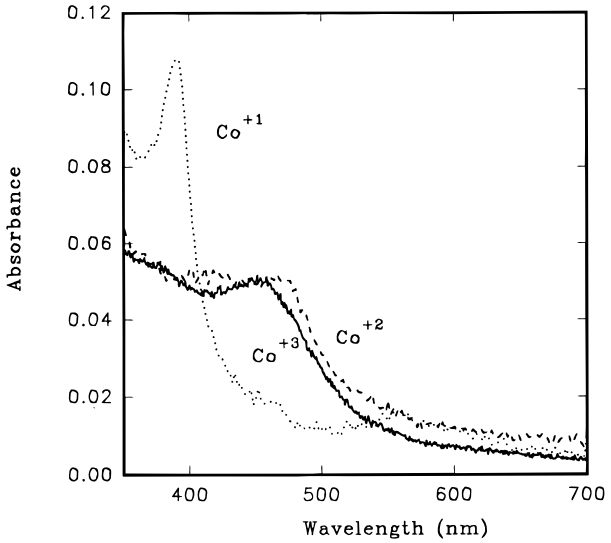

FIGURE 2: UV−visible spectra of the C20A mutant CFeSP in its three oxidation states. The as-isolated CFeSP in the cob(II)amide state (0.3 mg/mL) (- - -) was reduced by adding a 100-fold molar excess of titanium(III) citrate at pH 7.6 and removing the Ti with a Penefsky column (•••). The spectrum for the methylated enzyme was obtained by treating the reduced enzyme with CH_3-H_4 folate (—).

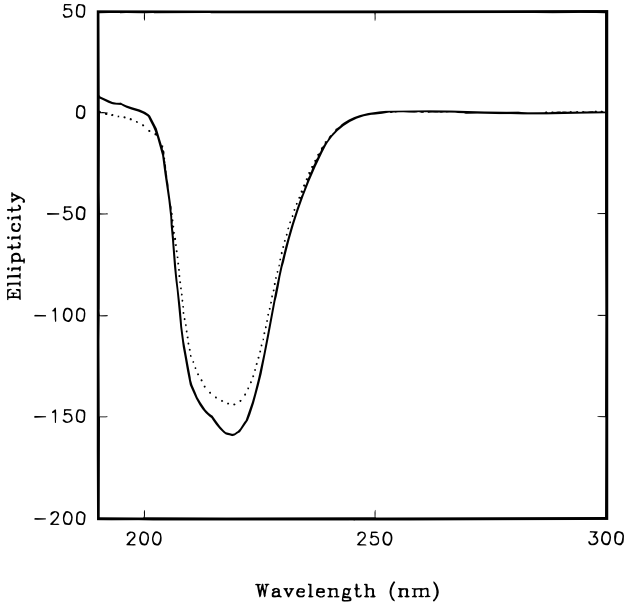

FIGURE 3: CD spectra of the oxidized wild type (—) and C20A (- - -) CFeSP in the UV region. The samples were equilibrated in 5 mM phosphate buffer, pH 7.6, after oxidation with excess thionine and removal of the excess thionine by repeated dilution using a microcon unit with a YM 30 membrane. The sample was exchanged repeatedly with 5 mM phosphate buffer, pH 7.6, and then made up to a concentration of 10 μM in a final volume of 1 mL.

intensities of the characteristic absorption peaks at 369, 542, and 584 nm were used to determine that the purified C20A variant contained 1.0 mol of cobamide/mol of heterodimeric protein.

The CD spectra of the oxidized variant and wild-type enzymes (Figure 3) show a negative band around 230 nm. The close similarity of the spectra in terms of both morphology and intensity provides convincing evidence that few changes have occurred in the secondary structure of the protein as a result of conversion of the 4Fe to a 3Fe cluster.

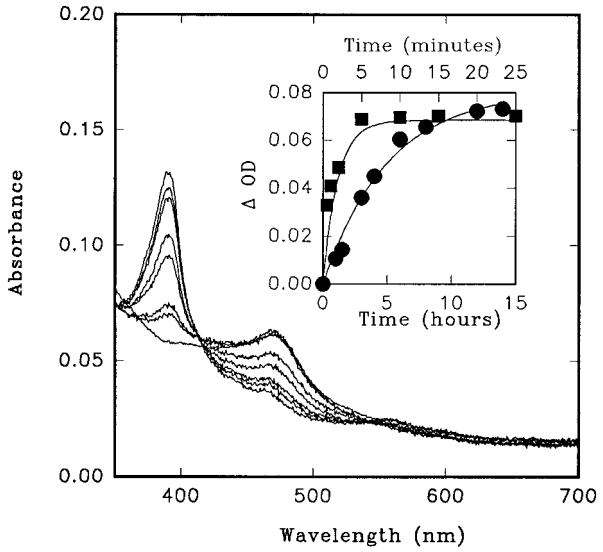

FIGURE 4: Reduction of Co(II) to Co(I) by CODH/ACS and CO. Reduction of the cob(II)amide state of the variant at 55 °C on the hour scale (at 0, 1, 1.5, 3, 4, 6, 8, and 14 h) and the wild-type CFeSP at 25 °C on the minute scale (spectra not shown) was followed by monitoring the appearance of the 390 nm peak of cob(I)amide. Experimental details are described under Materials and Methods. Inset: Data were fit to a single-exponential equation and gave rate constants of 0.0032 ± 0.0005 min^{-1} at 55 °C for the C20A protein (●) and 0.88 ± 0.11 min^{-1} at 25 °C for the wild-type enzyme (■).

The spectrum of the C20A variant in its "as-isolated" state contains a major absorption band at 470 nm indicating that, like the wild-type protein, the cobalt is in the Co(II) form (*9*, *31*); in addition, broad, unresolved sulfur-to-iron charge-transfer bands centered at about 400 nm are contributed by the cluster. The spectrum is very similar to that of the as-isolated wild-type enzyme that contains base-off cob(II)amide and a [4Fe-4S] cluster in the oxidized (2+) redox state. Both metal centers of the wild-type protein can be reduced to their 1+ states by CO and CODH/ACS, by low potential reductants such as dithionite or Ti(III) citrate or by electrochemical reduction in the presence of redox mediators (*9*, *17*). This change is marked by the appearance of a sharp absorption peak at 390 nm due to cob(I)amide and a bleaching in the 350−400 nm region due to reduction of the FeS cluster from the 2+ to the 1+ state. However, when the C20A variant was treated with CO and CODH/ACS, the spectrum showed bleaching in the 400−450 nm region and an extremely slow increase in absorbance at 390 nm. This indicated that the cluster underwent rapid reduction but the cobamide did not.

We compared the rate of Co(II) reduction by CO and CODH in the absence of Fd for the wild-type C20A variant proteins (Figure 4). For the variant, the rate of Co(I) formation (0.0032 ± 0.0005 min^{-1}) was determined at 55 °C because at room temperature when we used concentrations of CODH/ACS that were appropriate to monitor the reduction of the wild-type enzyme, the reduction took several days. To determine the rate of reduction of the wild-type enzyme we decreased the temperature to 25 °C and observed a rate of 0.88 ± 0.11 min^{-1}. Anticipating an ∼8-fold reduction in the reduction rate due to the 30 deg drop in temperature, we also studied the reduction of the wild-type protein at 55 °C using an 8-fold lower concentration of CODH/ACS. The rate of Co(I) formation was 0.95 ± 0.12 min^{-1}, which was nearly the same as for the wild-type

enzyme at 25 °C. This indicates that reduction of the cob(II)amide of the C20A variant occurred ~2000-fold slower than that of the wild type enzyme. In contrast, variant could be rapidly reduced by Ti(III) citrate at pH 7.6 (Figure 2), which has a midpoint potential of −540 mV (pH 7.5) (*32*) or excess sodium dithionite (10 mM) at pH 7.5, where the midpoint potential is −450 mV (*33*).

The wild-type cob(I)amide form of the CFeSP can be methylated by methyl iodide or CH_3-H_4folate in the presence of MeTr to form methyl-cob(III)amide (*8*, *9*). This reaction is marked by the disappearance of the 390 nm absorption peak and the appearance of a broad absorption feature at 450 nm. The spectrum of the methylcob(III)amide state is characteristic of a base-off state, which is distinct from that of most corrinoid proteins—their major absorption band is centered at 520 nm because either a histidine or benzimidazole group are ligated to Co at the lower axial position. Even though the experiments described above indicated that the Co center of the C20A protein was not reduced by CODH/ACS and CO, we considered that the protein might still undergo methylation with methyl iodide or CH_3-H_4folate since these reactions are thermodynamically very favorable. For example, methionine synthase could be methylated by CH_3-H_4folate at potentials as high as −450 mV and by S-adenosyl-L-methionine at potentials as high as −200 mV, even though its Co(II/I) couple has a midpoint potential of −526 mV (*34*). However, when the C20A variant was first treated with CODH/ACS and CO and then with CH_3-H_4-folate and MeTr, there were no indications of formation of methyl-cob(III)amide. In addition, no spectral changes were observed when methyl iodide was added when CODH/ACS and CO were provided as the potential electron source. However, when the variant CFeSP was reduced with sodium dithionite or titanium citrate and then treated with methyl iodide (not shown) or CH_3-H_4folate and MeTr (Figure 2), spectral changes characteristic of the methyl−Co(III) state were apparent. As with the native protein, the absorption band is at 450 nm, not at 520 nm, strongly indicating that there is not an imidazole or benzimidazole group coordinated to the lower axial site.

EPR Spectroscopy of the CFeSP. The EPR spectrum of the as-isolated C20A variant at 77 K is nearly identical to that of the wild-type protein and is typical of low-spin "base-off" cob(II)alamin (Figure 5). The $g_{||}$ resonance is split into eight lines by hyperfine interaction with the cobalt nucleus. Both the variant and wild-type proteins exhibit a large cobalt hyperfine splitting pattern ($A_{||,Co}$ = 142 G) and lack the characteristic three-line superhyperfine splittings that are observed in corrinoid proteins that have a coordinated nitrogen from imidazole or benzimidazole. This characteristic feature of the EPR spectrum provoked the postulate that the cobalt center in this protein is in the unusual "base-off" structure (*9*). This proposal was consistent with electrochemical and spectroscopic studies reported later (*17*, *35*, *36*). Thus, the coordination environment of the C20A CFeSP appears to be identical to that of the wild-type protein—both lack an axial nitrogen donor ligand. Double integration of the Co(II) spectrum of the variant yielded a value of 0.9 spins mol^{-1} of dimeric enzyme.

The EPR spectrum of the as-isolated C20A variant at 10 K only showed the cobamide spectrum with no indication of the 3 Fe cluster, which is EPR active in its 1+ oxidized state. When the protein was oxidized with thionine ($E_o' = +80$ mV) (Figure 6), the Co(II) spectrum disappeared and a signal near $g = 2.00$ was observed that is characteristic of an oxidized [3Fe-4S] cluster. Double integration of the signal yielded a spin intensity of 1.1 ± 0.1 spins mol^{-1} of heterodimeric enzyme. This spectrum was absent at a temperature of 80 K indicating that its relaxation properties are similar to those of other 3Fe clusters. No signal from the corrin ring was observed for the thionine-treated enzyme because the cobalt is converted to the EPR-silent Co(III) state. Since the protein was isolated in the presence of DTT, these experiments indicated that the midpoint potential of the 1+/0 couple of the [3Fe-4S] cluster is between −200 and +80 mV. An EPR spectroelectrochemical titration was performed to determine the redox potential of the 3Fe cluster (Figure 6). The cluster was found to undergo a one-electron reversible redox process with a midpoint potential of −31 ± 4 mV, which is nearly 500 mV more positive than that of the Co(II/I) center (−504 mV). Therefore, reductive activation of the Co(II) center by the reduced 3Fe cluster would be highly unfavorable by ~ 45 kJ mol^{-1}.

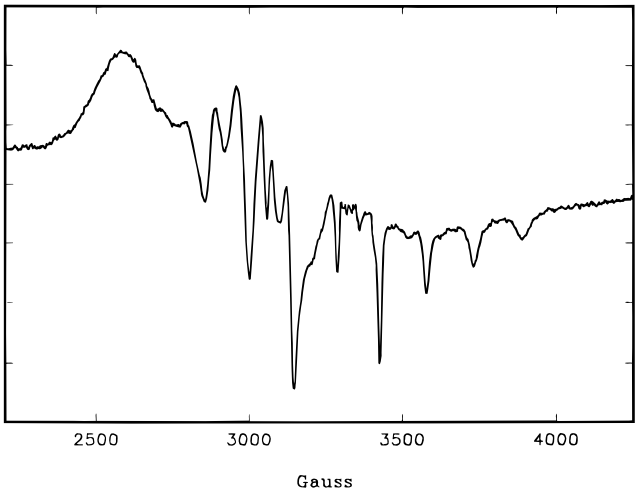

FIGURE 5: EPR spectrum of the C20A variant CFeSP. The isolated enzyme (60 μM) was in buffer containing 50 mM Tris-HCl buffer, pH 7.6. Spin integration of the sample gave a value of 0.9 spins mol^{-1} of enzyme. EPR conditions: temperature, 80 K; microwave frequency, 9.445 GHz; microwave power, 5 mW; modulation amplitude, 9.96 G; modulation frequency, 100 kHz; receiver gain, 2×10^4.

Enzymatic Measurements of the C20A Variant. In the single turnover reactions described above, it was shown that the C20A protein could not be methylated by CH_3-H_4folate or methyl iodide using CO and CODH/ACS as the electron donor regardless of whether Fd was present or not. The equilibrium constant for methylation of the cobamide center of the CFeSP in the analogous methanogenic multienzyme complex by methyltetrahydromethanopterin (a close analogue of CH_3-H_4folate) was determined to be 5.5 (*37*). It was important to determine the enzymatic properties of the C20A CFeSP under steady-state conditions, especially when a sufficient thermodynamic driving force is present. The formation of acetyl-CoA from CH_3-H_4folate, CO, and CoA is a highly exergonic reaction, with a K_{eq} of ~ 10^{11} (*38*). Therefore, we compared the rate of acetyl-CoA synthesis from CH_3-H_4folate, CO, and CoA between the C20A variant and wild-type CFeSPs as methyl carrier (Table 1). When this reaction was performed at very high concentrations of

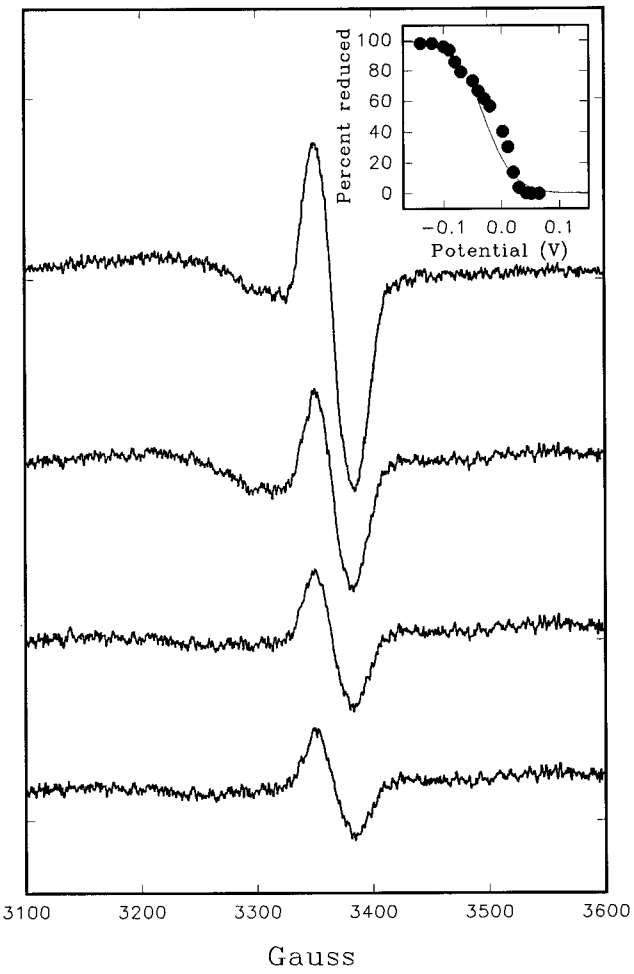

FIGURE 6: EPR spectroelectrochemical titration of the [3Fe-4S]$^{+/0}$ couple. Representative EPR spectra of the [3Fe-4S] cluster of the C20A variant CFeSP (50 μM) at +65, +11, −20, and −42 mV are shown. The protein was in a solution containing 50 mM Tris-HCl, pH 7.6, and redox dyes as described in Materials and Methods. The EPR conditions were the same as in Figure 5 except that the temperature was 10 K and the microwave power was 0.5 mW. Spin integration of the thionine-oxidized sample gave a value of 1.1 spins mol^{-1} of enzyme. Inset: The midpoint potential was determined by fitting the data to the Nernst equation to be −31 ± 4 mV. The value of n was 1.2 ± 0.2.

Table 1

conditions for acetyl-CoA synthesis from CH_3-H_4folate, CO, and CoA	rate ((μmol/min)/mg)	
	wild-type	C20A variant
A. limiting CODH/ACS		
plus ferredoxin	1.1 ± 0.02	0[a]
minus ferredoxin	0.17 ± 0.02	<0.007
B. limiting CODH/ACS + titanium citrate		
plus ferredoxin	0.89 ± 0.07	0.85 ± 0.06
minus ferredoxin	0.12 ± 0.01	0.13 ± 0.01

[a] The rates with the C20A protein and with the control reaction lacking any CFeSP were 0.032 ± 0.005 and 0.030 ± 0.003 (μmol/min)/mg, respectively.

MeTr and CFeSP and limiting amounts of CODH/ACS in the absence of Fd, the rate of acetyl-CoA synthesis with the wild-type recombinant protein was similar to the rate determined earlier for the native CFeSP isolated from *C. thermoaceticum* (0.12 μmol min^{-1} mg^{-1}) (*28*). This is consistent with earlier studies in which it was concluded that

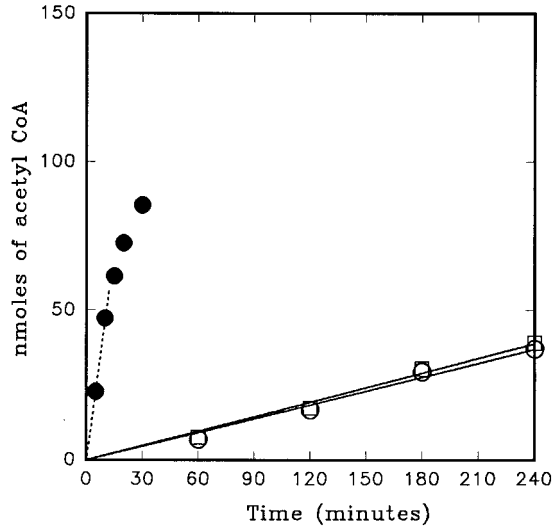

FIGURE 7: Acetyl-CoA synthesis from CH_3-H_4folate. The assay for the synthesis of acetyl-CoA was performed at 55 °C in the presence of Fd as described in Materials and Methods. The specific activities calculated from the lines shown were 1.1 ± 0.02, 0.03 ± 0.01, and 0.03 ± 0.01 μmol min^{-1} mg^{-1} for the wild type (●), control (○), and C20A (□) enzymes.

the recombinant and native proteins had identical properties (*10*). When the C20A variant was substituted for the wild-type enzyme in this reaction, no activity was detected even when the reaction was performed overnight (Table 1). Therefore, only an upper limit for the rate with the variant could be estimated—it was at least 2000-fold less active than the wild-type protein in transferring the methyl group from CH_3-H_4folate to CODH/ACS.

We considered that Fd might replace the role of the [4Fe-4S] cluster of the C20A variant and ran the acetyl-CoA synthesis assay under identical conditions with limiting CODH but including 3.3 μM FdII. As above, the rate of acetyl-CoA synthesis with the wild-type CFeSP (1.1 μmol min^{-1} mg^{-1}) was approximately equal to that determined earlier for the native protein (0.87 μmol min^{-1} mg^{-1}) (*28*); however, when the C20A variant replaced the wild-type protein, the rate of acetyl-CoA synthesis was 0.032 ± 0.005 μmol min^{-1} mg^{-1}. As shown earlier (*10*), it is extremely difficult to remove all traces of CFeSP from CODH/ACS preparations. When the CFeSP was removed in a control reaction mixture the reaction rate was determined to be 0.030 ± 0.003 μmol min^{-1} mg^{-1} (Figure 7). The difference between the reaction with the C20A variant and the control, therefore, is only 0.002 μmol min^{-1} mg^{-1}, which is within the standard error of measurement. Therefore, even when a strong thermodynamic driving force was provided during a steady-state reaction, the 3Fe-containing C20A variant CFeSP was at least 550-fold less active than the wild-type protein and the role of the low-potential 4Fe cluster could not be replaced by Fd.

Above it was shown that the Co center of the C20A variant could be reduced chemically. Therefore, when the acetyl-CoA synthesis reaction was performed in the presence of Ti(III) citrate with limiting amounts of CODH/ACS (CODH/ACS and CO are still required because CO serves as the carbonyl group of acetyl-CoA), the C20A variant and the wild-type CFeSPs were equally proficient (Table 1B).

It was demonstrated earlier that when methyl iodide was used as the methyl donor, the Co(I) center was directly

methylated, bypassing the requirement for MeTr (*18*). CODH/ACS could not be directly methylated by methyl iodide; the only methyl donor that has been found to react with CODH/ACS is the methylated CFeSP. Reactions involving methyl iodide could not be performed at 55 °C because of its high volatility. The rate of acetyl-CoA synthesis from ^{14}C-methyl iodide, CO, and CoA in the presence of the wild-type CFeSP and CODH/ACS at 25 °C was 0.11 ± 0.01 μmol min^{-1} mg^{-1}. Since the rate of acetyl-CoA synthesis doubles with each 10 °C increase in temperature, the specific activity expected at 55 °C would be ~0.9 μmol min^{-1} mg^{-1}, which is almost the same as the rate of acetyl-CoA synthesis from CH_3-H_4folate. When the same reaction was performed with the C20A protein, acetyl-CoA was not detected after 30 min of reaction time.

Methylation of the CFeSP by CH_3-H_4 folate is a reversible reaction (*19*). In the reverse reaction, H_4folate appears to perform a nucleophilic attack on methyl−Co(III) to form Co(I). When the methylated C20A CFeSP was reacted with H_4folate, the k_{cat} for CH_3-H_4folate formation at pH 5.8 was determined to be 0.08 s^{-1}, in agreement with a previously determined value of >0.02 s^{-1} (*19*). Therefore, transfer of the methyl group from CH_3-CFeSP to H_4folate in a single turnover reaction does not require a low-potential FeS cluster.

These combined results strongly indicate that the cluster is involved in reductive activation of the cob(II)amide to the Co(I) state and that it plays no role in the turnover cycle involving transfer of the methyl group from CH_3-H_4folate to cob(I)amide. This further indicates that, during catalysis, electron transfer reactions involving the FeS cluster do not occur. This conclusion is consistent with the commonly accepted model for the MeTr reaction in which the methyl group is transferred as a cation in an S_N2 mechanism.

It remained possible that the FeS cluster of the CFeSP could be involved in the methyl transfer from the methylated CFeSP to CODH/ACS. For example, one possible mechanism for this reaction is one-electron transfer from a reduced FeS cluster to methyl-cob(III)amide to form methyl-cob(II)amide which could undergo homolysis to generate cob(I)amide and a methyl radical that could react with CODH/ACS. The role of the FeS in this reaction was tested by performing acetyl-CoA synthesis from the methylated CFeSP, CO, Fd, and CoA in the presence of CODH/ACS and in the absence of any additional electron donor (Figure 8). In this single turnover reaction, the rate of acetyl-CoA synthesis at 25 °C was found to be 0.14 and 0.13 μmol min^{-1} mg^{-1} for the wild type and variant CFeSP, respectively. These results indicate that the low-potential 4Fe cluster in the CFeSP is not involved in transfer of the methyl group from methyl-cob(III)amide to CODH/ACS. Therefore, the only apparent role of the cluster is for reductive activation of the cobalt site when the CFeSP is in the cob(II)amide state.

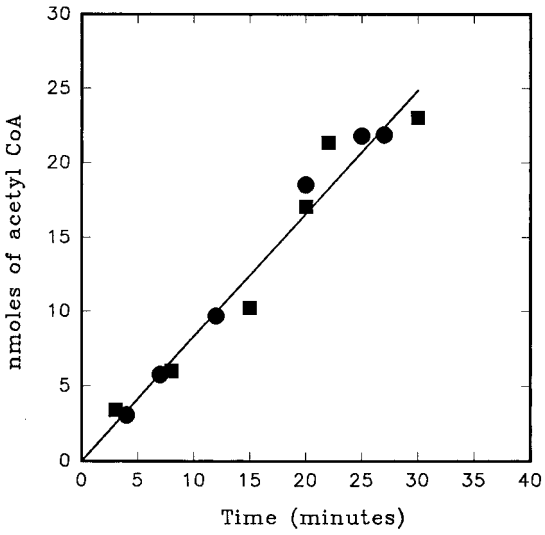

FIGURE 8: Synthesis of acetyl-CoA from the methylated CFeSP. The reaction contained CODH/ACS, $^{14}CH_3$-CFeSP, Fd, and CoA and was performed at pH 5.8 and 25 °C as described in Materials and Methods. The linear fit to the data resulted in rates of 0.141 ± 0.014 μmol min^{-1} mg^{-1} and 0.138 ± 0.006 μmol min^{-1} mg^{-1} for the variant (■) and wild type (●) enzymes.

DISCUSSION

The CFeSP from *C. thermoaceticum* was the first protein reported to contain both a corrinoid and an iron sulfur cluster (*9*). Biophysical characterization of the cluster demonstrated that it was of the [4Fe-4S]$^{2+/+}$ type (*9*). When the gene encoding the large subunit of the CFeSP was sequenced, an arrangement, $C-X_2-C-X_4-C$, near the N terminus was identified (*10*). This motif is similar to that of the "group 2" Fe/S proteins, indicating that the cluster is in the large subunit and that these cysteine residues are involved in ligating iron atoms in the cluster. This hypothesis was tested by the mutagenesis experiments reported here in which the second of these cysteine residues (C20) was converted to alanine. The EPR spectra and redox properties of the C20A variant strongly indicate that this mutation converts the 4Fe cluster into a [3Fe-4S] center, confirming that the cluster is in the large subunit and that the sulfur atom of C20 is involved in cluster ligation. This conclusion is expected to extend to the conserved motif in the CFeSP from aceticlastic methanogens.

The kinetic and spectroscopic (UV−visible, EPR, and CD) properties of the C20A variant protein were compared with those of the wild-type protein to probe the function of the cluster in catalysis. Our studies indicate that there were no major secondary or tertiary structural rearrangements accompanying the replacement of C20 by alanine and the resulting 4Fe to 3Fe cluster conversion. Our results strongly indicate that the [4Fe-4S] cluster plays a role in reductive activation of the Co center. This conclusion is based on the severely damaged capacity of the Co center of the C20A variant to undergo reduction by physiological reductants or methylation by CH_3-H_4folate or methyl iodide under conditions that require reductive activation. In addition, it was shown that the cluster is not involved in the catalytic cycles of methyl transfer from CH_3-H_4folate to the CFeSP or from the methylated CFeSP to CODH/ACS. When chemical reductants were present, the C20A variant was as efficient as the wild-type protein in its ability to be methylated by methyl iodide or CH_3-H_4folate. In addition, the methylated C20A variant could transfer its methyl group to H_4folate or to CODH/ACS as proficiently as the wild type protein. Therefore, when a 3Fe cluster is present to replace the low potential 4Fe cluster, the CFeSP appears to be blocked from undergoing activation. Our interpretation of the reason for this blockage is outlined in Figure 1. We propose that the pathway of electron flow is from reduced CODH to the FeS cluster of the CFeSP and then finally to the Co center. Ferredoxin could not replace the function of this cluster.

However, chemical reductants could rescue the activity of the C20A variant indicating that the Co center has enough solvent exposure to be accessible to these reagents.

Figure 1 outlines both the catalytic and activation cycles of the CFeSP. During catalysis, we propose that the CFeSP forms complexes with CODH/ACS and MeTr. Evidence for the CODH/ACS−CFeSP complex in *C. thermoaceticum* is based on their coelution under some chromatographic conditions (*8*, *39*) and the identification of a specific cysteine residue in the α subunit that can form a disulfide link between the two proteins (*39*). In methanoarchaea, the interaction between these proteins is even tighter—a five-protein complex that has CODH, ACS, CFeSP, and MeTr activities has been isolated from *Ms. thermophila* (*40*) and *Ms. barkeri* (*41*−*43*). Figure 1 also proposes that CODH/ACS and CH_3-H_4folate/MeTr have to compete for interaction with the CFeSP. This is based on the dual roles of the Co center of the CFeSP—at every round of catalysis, it has to bind CH_3-H_4folate to append the methyl group to Co at the upper axial position and then center A of ACS has to come within bonding distance of the methyl group to perform an S_N2 attack. We suggest that ligation and oxidation states of the cluster and the Co center control whether the MeTr-CFeSP or the CODH/ACS-CFeSP complexes are favored. In the proposal, the Co(I) state favors interaction with MeTr and CH_3-H_4folate; whereas, the methyl−Co(III) state favors CFeSP-ACS interaction. As shown in the scheme, the FeS cluster does not appear to be involved in either of the two catalytic cycles of successive methylation and demethylation.

The results reported here indicate that the FeS cluster is required only in the reductive activation cycle that couples the oxidation of substrates such as CO to the reduction of Co(II). Deleterious oxidation of the cluster and the Co center is bound to occur during cell growth since the midpoint potentials for the II/I couples of these cofactors are below −500 mV. When this happens, the only way that acetyl-CoA can be synthesized is by supplying a low-potential electron to regenerate the Co(I) state. Our results strongly suggest that direct electron transfer from the CODH subunit of CODH/ACS center directly to the Co center on the CFeSP is unfavorable. Instead, the FeS cluster is present to relay electrons from CODH to Co. Therefore, we propose that when Co is in the 2+ oxidation state, a complex between the FeS subunit of the CFeSP and the CODH subunit of CODH/ACS is favored. This complex would be expected to lead to an optimum geometry and distance between the Fe−S clusters on both proteins. Although further studies are required to fully understand the interactions between the CFeSP and CODH/ACS, we speculate that the interaction is between cluster B of CODH and the 4Fe cluster of the CFeSP, since it has been shown that cluster B communicates with external electron acceptors and that cluster B is reduced by cluster C at much faster rates (*44*) than the rates of reduction of the cobalt center of the CFeSP by CODH and CO measured here. Once Co(I) is formed, the binding affinity for CODH/ACS is expected to be reduced as the affinity for MeTr/CH_3-H_4folate increases.

The scenario just described is reminiscent of the activation and catalytic cycles of several other corrinoid-containing methyltransferases, including methionine synthase. Its catalytic cycle involves the methylation of a bound Co(I) center by CH_3-H_4folate to form methylcobalamin followed by transfer of the methyl group to homocysteine to form methionine and Co(I). When the Co(I) center undergoes oxidation to the inactive Co(II) state, return to the catalytic cycle is apparently accomplished by a reductive methylation mechanism in which the thermodynamically unfavorable reduction of Co(II) to Co(I) is coupled to the demethylation of *S*-adenosyl-L-methionine (AdoMet) forming methylcobalamin (*34*). For the *E. coli* system, flavodoxin serves as the electron donor. In humans, the electron donor may include a microsomal electron-transfer system like cytochrome P_{450} (*45*). The structures of the AdoMet (*46*) and the cobalamin binding domains (*47*) of the *E. coli* methionine synthase have been solved, and a hypothesis has been framed to explain how only AdoMet can serve as the methyl donor for the reactivation reaction and CH_3-H_4folate for the catalytic cycle. It was proposed that the catalytic and activation cycles are turned off and on by major conformational changes that accomplish the alternating physical separation and approach of the reactants, AdoMet and CH_3-H_4folate (*46*).

There exist analogous proteins from methanoarchaea. One type transfers a methyl group from methyltetrahydrosarcinopterin or methyltetrahydromethanopterin (CH_3-H_4MPT), which are analogues of CH_3-H_4folate, to coenzyme M to form methyl-CoM, the direct precursor or methane. In *M. thermoautotrophicum* (*48*−*51*) and *M. mazei* strain Gö1, this reaction is linked to the translocation of sodium ions, which forms a sodium gradient that is linked to ATP synthesis (*52*−*54*, *50*, *55*, *56*). This complex system has been purified from *M. thermoautotrophicum* strain Marburg (*51*) and *M. mazei* strain Gö1 (*56*). Another type of methyltransferase system is present in methanol- or methylamine-grown *M. barkeri* (*57*−*59*) that involves a three-component system including (i) a protein that binds and transfers the methyl group from a methylated substrate to (ii) a cobamide-containing protein, forming methyl-cobamide, and (iii) a protein that transfers the methyl group from the methylated class 2 corrinoid protein to CoM (*60*, *51*, *58*, *61*−*65*). The latter component is a zinc metalloenzyme, and on the basis of recent results, it was suggested that catalysis is promoted by binding of CoM by S coordination to zinc and electrostatic interaction of the sulfonate with a cationic group on the enzyme (*59*). Zn also appears to be important in activation of homocysteine in methionine synthase (*66*).

Therefore, it appears that among the different cobalamin-dependent methyltransferases, the catalytic cycles are similar and involve two half-reactions: (i) nucleophilic attack of Co(I) on CH_3-H_4folate, or its methanogenic analogue; (ii) nucleophilic attack of organic thiolates (CoM, homocysteine) or a low potential NiFeS complex of CODH/ACS on bound methyl−Co(III). There exist several variations on the theme of one-electron reductive reactivation of the inactive Co(II) enzymes. Separate subunits are present on the methanogenic and acetogenic CFeSPs that are analogous to flavodoxin for the *E. coli* methionine synthase. The reactivation mechanisms for the systems that transfer methyl groups to CoM have not been studied, although it is clear that the sodium-ion-translocating enzymes contain low-potential FeS clusters (*55*) that could play a role in activation. The reductive activation system for the human cobalamin-dependent methionine synthase shares with *E. coli* its AdoMet dependence yet has a completely different, but still undefined, electron-transfer component (*45*). The methyltransferases from the

strict anaerobes do not require AdoMet. Probably, the redox potential in growing anaerobic cells is low enough that this extra thermodynamic push would be extraneous. The existence of a low potential reductant in the cell indeed has only the "potential" to activate. The studies described here have shown that placing the C20A variant CFeSP in solution with a large excess of its physiological reductant was not effective; the low-potential [4Fe-4S] cluster was essential to direct these low-potential electrons to the appropriate destination.

SUPPORTING INFORMATION AVAILABLE

UV−visible spectra of the wild-type CFeSP in its three oxidation states (1 page). Ordering information is given on any current masthead page.

REFERENCES

1. Ferry, J. G. (Ed.) (1993) in *Methanogenesis: ecology physiology, biochemistry & genetics*, p 536, Chapman & Hall, London.
2. Drake, H. L. (Ed.) (1994) in *Acetogenesis* Vol., p 647, Chapman and Hall, New York.
3. Ragsdale, S. W. (1997) *BioFactors 9*, 1−9.
4. Thauer, R. (1997) *Anton Leeuwenhoek Int. J. Gen. Microbiol. 71*, 21−32.
5. Ljungdahl, L. G. (1986) *Annu. Rev. Microbiol. 40*, 415−450.
6. Ragsdale, S. W. (1991) *CRC Crit. Rev. Biochem. Mol. Biol. 26*, 261−300.
7. Ragsdale, S. W., and Kumar, M. (1996) *Chem. Rev. 96*, 2515−2539.
8. Hu, S.-I., Pezacka, E., and Wood, H. G. (1984) *J. Biol. Chem. 259*, 8892−8897.
9. Ragsdale, S. W., Lindahl, P. A., and Münck, E. (1987) *J. Biol. Chem. 262*, 14289−14297.
10. Lu, W.-P., Schiau, I., Cunningham, J. R., and Ragsdale, S. W. (1993) *J. Biol. Chem. 268*, 5605−5614.
11. Abbanat, D. R., and Ferry, J. G. (1991) *Proc. Natl. Acad. Sci. U.S.A. 88*, 3272−3276.
12. Jablonski, P. E., Lu, W.-P., Ragsdale, S. W., and Ferry, J. G. (1993) *J. Biol. Chem. 268*, 325−329.
13. Roberts, D. L., James-Hagstrom, J. E., Smith, D. K., Gorst, C. M., Runquist, J. A., Baur, J. R., Haase, F. C., and Ragsdale, S. W. (1989) *Proc. Natl. Acad. Sci. U.S.A. 86*, 32−36.
14. Ram, M. S., and Riordan, C. G. (1995) *J. Am. Chem. Soc. 117*, 2365−2366.
15. Ram, M. S., Riordan, C. G., Yap, G. P. A., LiableSands, L., Rheingold, A. L., Marchaj, A., and Norton, J. R. (1997) *J. Am. Chem. Soc. 119*, 1648−1655.
16. Ragsdale, S. W., and Riordan, C. G. (1996) *J. Bioinorg. Chem. 1*, 489−493.
17. Harder, S. A., Lu, W.-P., Feinberg, B. F., and Ragsdale, S. W. (1989) *Biochemistry 28*, 9080−9087.
18. Lu, W.-P., Harder, S. R., and Ragsdale, S. W. (1990) *J. Biol. Chem. 265*, 3124−3133.
19. Zhao, S., Roberts, D. L., and Ragsdale, S. W. (1995) *Biochemistry 34*, 15075−15083.
20. Stiefel, E. I., and George, G. N. (1994) in *Bioinorganic Chemistry* (Bertini, I., Gray, H. B., Lippard, S. J., and Valentine, J. S., Eds.) pp 365−463, University Science Books, Mill Valley, CA.
21. Andreesen, J. R., Schaupp, A., Neurater, C., Brown, A., and Ljungdahl, L. G. (1973) *J. Bacteriol. 114*, 743−751.
22. Ragsdale, S. W., Clark, J. E., Ljungdahl, L. G., Lundie, L. L., and Drake, H. L. (1983) *J. Biol. Chem. 258*, 2364−2369.
23. Elliott, J. I., and Ljungdahl, L. G. (1982) *J. Bacteriol. 151*, 328−333.
24. Elliott, J. I., and Brewer, J. M. (1978) *Arch. Biochem. Biophys. 190*, 351−357.
25. Horton, R. M., Ho, S. N., Pullen, J. K., Hunt, H. D., Cai, Z., and Pease, L. R. (1993) *Methods Enzymol. 217*, 270−279.
26. Harder, S. A., Feinberg, B. F., and Ragsdale, S. W. (1989) *Anal. Biochem. 181*, 283−287.
27. Ljungdahl, L. G., LeGall, J., and Lee, J.-P. (1973) *Biochemistry 12*, 1802−1808.
28. Roberts, J. R., Lu, W.-P., and Ragsdale, S. W. (1992) *J. Bacteriol. 174*, 4667−4676.
29. Drake, H. L., Hu, S.-I., and Wood, H. G. (1981) *J. Biol. Chem. 256*, 11137−11144.
30. Penefsky, H. S. (1977) *J. Biol. Chem. 252*, 2891−2899.
31. Lexa, D., Savéant, J.-M., and Zickler, J. (1977) *J. Am. Chem. Soc. 99*, 2786.
32. Zehnder, A. J. B., and Wuhrmann, K. (1976) *Science 194*, 1165−1166.
33. Mayhew, S. G. (1978) *Eur. J. Biochem. 85*, 535−547.
34. Banerjee, R. V., Harder, S. R., Ragsdale, S. W., and Matthews, R. G. (1990) *Biochemistry 29*, 1129−1135.
35. Wirt, M. D., Sagi, I., and Chance, M. R. (1992) *Biophys. J. 63*, 412−417.
36. Wirt, M. D., Kumar, M., Ragsdale, S. W., and Chance, M. R. (1993) *J. Am. Chem. Soc. 115*, 2146−2150.
37. Grahame, D. A., and Demoll, E. (1996) *J. Biol. Chem. 271*, 8352−8358.
38. Grahame, D. A., and Demoll, E. (1995) *Biochemistry 34*, 4617−4624.
39. Shanmugasundaram, T., Sundaresh, C. S., and Kumar, G. K. (1993) *FEBS Lett. 326*, 281−284.
40. Terlesky, K. C., Nelson, M. J. K., and Ferry, J. G. (1986) *J. Bacteriol. 168*, 1053−1058.
41. Grahame, D. A., and Stadtman, T. C. (1987) *J. Biol. Chem. 262*, 3706−3712.
42. Grahame, D. A. (1991) *J. Biol. Chem. 266*, 22227−22233.
43. Grahame, D. A. (1993) *Biochemistry 32*, 10786−10793.
44. Seravalli, J., Kumar, M., Lu, W.-P., and Ragsdale, S. W. (1997) *Biochemistry 36*, 11241−51.
45. Banerjee, R. (1997) *Chem. Biol. 4*, 175−186.
46. Dixon, M. M., Huang, S., Matthews, R. G., and Ludwig, M. (1996) *Structure 4*, 1263−1275.
47. Drennan, C. L., Huang, S., Drummond, J. T., Matthews, R. G., and Ludwig, M. L. (1994) *Science 266*, 1669−1674.
48. Gärtner, P., Ecker, A., Fischer, R., Linder, D., Fuchs, G., and Thauer, R. K. (1993) *Eur. J. Biochem. 213*, 537−545.
49. Gartner, P., Weiss, D. S., Harms, U., and Thauer, R. K. (1994) *Eur. J. Biochem. 226*, 465−472.
50. Weiss, D. S., Gartner, P., and Thauer, R. K. (1994) *Eur. J. Biochem. 226*, 799−809.
51. Harms, U., Weiss, D. S., Gartner, P., Linder, D., and Thauer, R. K. (1995) *Eur. J. Biochem. 228*, 640−648.
52. Becher, B., Müller, V., and Gottschalk, G. (1992) *FEMS Microbiol. Lett. 91*, 239−244.
53. Becher, B., Müller, V., and Gottschalk, G. (1992) *J. Bacteriol. 174*, 7656−7660.
54. Müller, V., and Gottschalk, G. (1994) in *Acetogenesis* (Drake, H. L., Ed.) pp 127−156, Chapman and Hall, New York.
55. Lu, W.-P., Becher, B., Gottschalk, G., and Ragsdale, S. W. (1995) *J. Bacteriol. 177*, 2245−2250.
56. Lienard, T., Becher, B., Marschall, M., Bowien, S., and Gottschalk, G. (1996) *Eur. J. Biochem. 239*, 857−864.
57. Grahame, D. A. (1989) *J. Biol. Chem. 264*, 12890.
58. Ferguson, D. J., Krzycki, J. A., and Grahame, D. A. (1996) *J. Biol. Chem. 271*, 5189−5194.
59. Leclerc, G. M., and Grahame, D. A. (1996) *J. Biol. Chem. 271*, 18725−18731.
60. Burke, S. A., and Krzycki, J. A. (1995) *J. Bacteriol. 177*, 4410−4416.
61. Harms, U., and Thauer, R. K. (1996) *Eur. J. Biochem. 235*, 653−659.
62. Paul, L., and Krzycki, J. A. (1996) *J. Bacteriol. 178*, 6599−6607.
63. Tallant, T. C., and Krzycki, J. A. (1996) *J. Bacteriol. 178*, 1295−1301.
64. Ferguson, D. J., and Krzycki, J. A. (1997) *J. Bacteriol. 179*, 846−852.
65. Sauer, K., Harms, U., and Thauer, R. K. (1997) *Eur. J. Biochem. 243*, 670−677.
66. Gonzalez, J. C., Peariso, K., Penner-Hahn, J. E., and Matthews, R. G. (1996) *Biochemistry 35*, 12228−12234.

BI9727996